



Characterization of acoustofluidic geometric traps by means of defocus particle tracking

Rossi, M.; Joergensen, J. H.; Bruus, H.

Published in:

Proceedings of the 20th International Symposium on Application of Laser and Imaging Techniques to Fluid Mechanics

Publication date:

2022

Document Version

Publisher's PDF, also known as Version of record

[Link back to DTU Orbit](#)

Citation (APA):

Rossi, M., Joergensen, J. H., & Bruus, H. (2022). Characterization of acoustofluidic geometric traps by means of defocus particle tracking. In *Proceedings of the 20th International Symposium on Application of Laser and Imaging Techniques to Fluid Mechanics* Instituto Superior Técnico.

General rights

Copyright and moral rights for the publications made accessible in the public portal are retained by the authors and/or other copyright owners and it is a condition of accessing publications that users recognise and abide by the legal requirements associated with these rights.

- Users may download and print one copy of any publication from the public portal for the purpose of private study or research.
- You may not further distribute the material or use it for any profit-making activity or commercial gain
- You may freely distribute the URL identifying the publication in the public portal

If you believe that this document breaches copyright please contact us providing details, and we will remove access to the work immediately and investigate your claim.

Characterization of acoustofluidic geometric traps by means of defocus particle tracking

M. Rossi^{1,*}, J. H. Joergensen¹, H. Bruus¹

1: Department of Physics, Technical University of Denmark, DTU Physics Building 309, DK-2800 Kongens Lyngby, Denmark

*Corresponding author: rossi@fysik.dtu.dk

Keywords: Defocus Particle Tracking, 3D PTV, Microfluidics, Acoustofluidics

ABSTRACT

In this work we used the General Defocusing Particle Tracking method to measure the three-dimensional trajectories of 10- μm -diameter polystyrene beads moving inside a micro-acoustofluidic device. The aim is to measure the change in acoustic energy density induced by localized modifications of the channel geometry. The measurements were performed in a glass capillary tube with a rectangular cross-section of $2.0 \times 0.2 \text{ mm}^2$. The wall thickness of the capillary tube is $140 \mu\text{m}$ and it was locally increased by gluing a glass slide with a thickness of $100 \mu\text{m}$. The acoustic energies at five different frequencies around the expected resonant frequency have been estimated for the single-glass and double-glass region from the measured particle paths. The results showed a down-shift of the resonant frequency in the double-glass zone, as expected from theoretical predictions. This approach can be used to create multiple acoustofluidic traps based on simple geometrical modifications of the microchannel.

1. Introduction

Microscale acoustofluidics enables the manipulation of particles or cells by means of acoustic radiation forces that push them to the pressure nodes (or antinodes) created by a resonant standing wave in a liquid-filled cavity (Bruus, 2012). This approach has important applications in lab-on-a-chip systems for instance for trapping particles and performing automatized analysis (Evander et al., 2015; Lim et al., 2021). Velocimetry methods have played a major role in this research field for understanding the physics of acoustic streaming phenomena and validating numerical predictions (Muller et al., 2013; Karlsen et al., 2018). The major challenges of flow measurements in acoustofluidics are the sub-millemetric dimensions of the devices that allow often only a single optical access through a microscope, and the strongly three-dimensional nature of the flows. For these reasons, single-camera 3D-PTV methods, such as methods based on defocusing or astigmatism (Barnkob et al., 2015; Cierpka et al., 2011), have been particularly successful in this field. In this work we use the General Defocusing Particle Tracking method (Barnkob et al., 2015) to estimate the acoustic energy density inside an acoustofluidic device, in which the thickness of the microchannel has been locally increased. The local thickness increase is expected to locally modify the resonant frequency. This approach could be useful for instance to create multiple acoustic traps in a chip driven by a single piezoelectric transducer.



2. Material and methods

The microfluidic device is composed by a 50-mm-long glass capillary tube with a 2-mm-wide, 0.2-mm-thick rectangular cross-section (CM scientific). The wall thickness of the capillary tube is 140 μm and it was locally increased by gluing a 1-mm-long, 100- μm -thick glass slide, as shown in the sketch in Fig. 1. A piezoelectric transducer (PZT) disk with diameter of 16 mm and thickness of 0.5 mm (Pz26, Meggit A/S) was glued on the capillary tube with UV glue. The resonant frequency was determined following the procedure described in Vitali et al. (2019), giving a value $f_{\text{res}} = 3.390$ MHz. The PZT was driven with a sinusoidal signal at a peak-to-peak voltage amplitude of 2 V (Digilent Analog Discovery 2).

We used ultra-pure water as working fluid and fluorescent polystyrene spheres with a diameter of 10 μm (Microparticles GmbH) as probing beads. Digital images of the beads in the fluids were taken using an epifluorescent microscope system equipped with a 5 \times objective lens (Zeiss AG) and a high-sensitivity sCMOS camera (pco.edge 5.5, PCO GmbH). The illumination was provided by a high-power LED (Solis-525C, Thorlabs Inc). A cylindrical lens with focal length of 500 mm was placed in front of the camera sensor to introduce an astigmatic aberration that was needed for the particle tracking method.

The three-dimensional position of the particles was determined using the General Defocusing Particle tracking method (GDPT) (Barnkob et al., 2015). This method relies on the different shape of particle images observed through a microscope objective with small depth of field. The different shapes correspond to defocusing patterns and are directly related to the particle distance from the focal plane (i.e. the depth position). GDPT uses a pattern recognition approach to match the par-

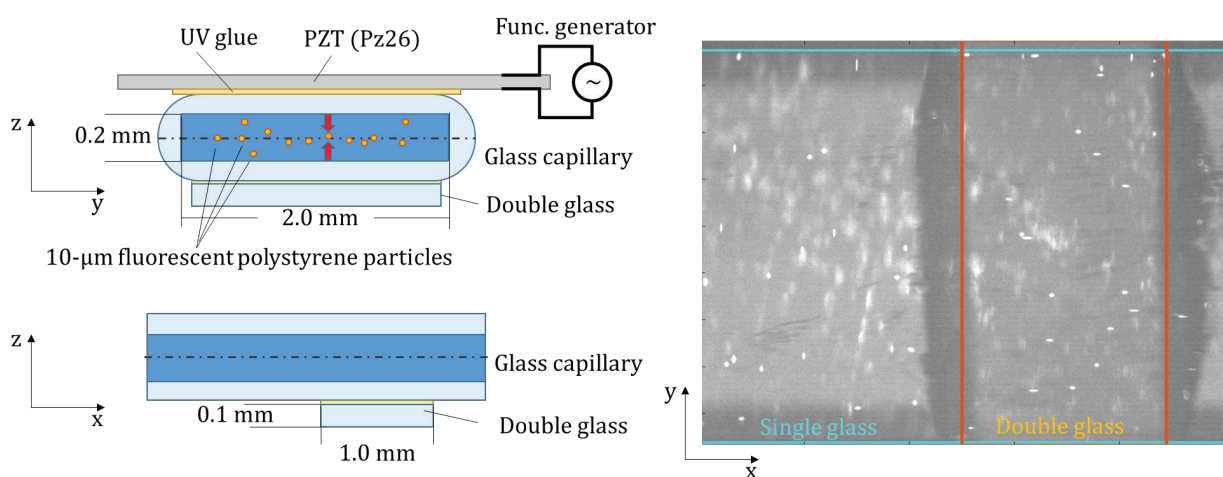


Figure 1. Left: Sketch of the acoustofluidic device consisting of a glass capillary tube with internal cross-section of $2.0 \times 0.2 \text{ mm}^2$. The ultrasound actuation is provided by a piezoelectric transducer glued on the capillary tube. The thickness of the wall is modified locally by gluing a 0.1-mm-thick glass slide. Right: Defocused particle images taken with a 5 \times microscope objective with a cylindrical lens in front of the camera sensor. The double-glass region is highlighted in orange.

ticle image shapes with their corresponding depth positions. The pattern recognition method is calibrated on a set of reference particle images taken at known depth positions. The detection of the particle image shape is improved by introducing a mild astigmatic aberration in the optical system (Barnkob et al., 2015; Cierpka et al., 2011). We used the open-source software *Defocus-Tracker* (Barnkob & Rossi, 2021) for image analysis and post-processing of the data.

3. Results

The GDPT measurements were carried out at five different operating frequencies, corresponding to 97%, 98%, 99%, 100%, and 101% of f_{res} . We chose those frequencies since the larger acoustic energy density was expected at $f = f_{\text{res}}$ in the single-glass zone, and at $f < f_{\text{res}}$ in the double-glass zone. For each experiment we followed the same measurement procedure: First, the microchannel was loaded with a fresh solution of ultra-pure water and polystyrene beads. Then, a two-way valve was used to short-circuit the microchannel and stop the flow. Then, we started the image recording, switched on the ultrasound after 2 seconds, and finally stopped the recording after 20 seconds.

The optical arrangement provided a total measurement depth of 400 μm with a lateral field of view of $2.8 \times 2.0 \text{ mm}^2$ that was sufficient to observe simultaneously the full depth of the channel, the double-glass zone and a portion of the single-glass zone. After image analysis, the 3D position

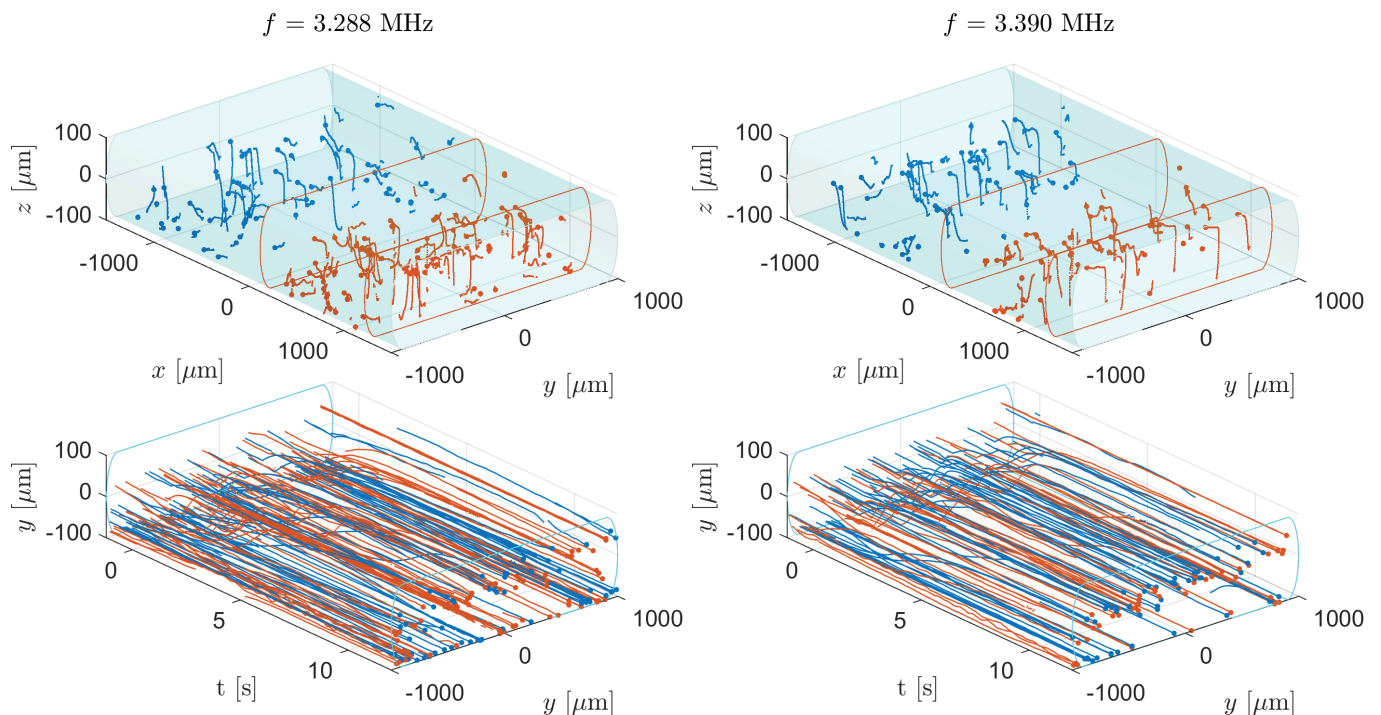


Figure 2. Example of 3D particle trajectories obtained at different frequencies. Top: particles in the measurement volume. Particles in the double-glass region are plotted in orange. Bottom: Cross-sectional particle position as a function of time. After the the ultrasound is switched on the particles move to the nodal plane.

of the particles was determined with an estimated uncertainty of 0.2 μm in the in-plane direction and 4 μm in the out-of-plane direction (Barnkob & Rossi, 2020). The tracking was performed using a simple nearest-neighbor scheme given the low particle density. A series of 3 experiments was performed for each frequency giving a total average of 200 valid trajectories for each case.

The 3D particle trajectories obtained for two frequencies are shown in Fig. 2. It should be noted that the polystyrene beads are slightly heavier than water ($\rho_{\text{PS}} = 1050 \text{ kg/m}^3$) and sediment with a sinking velocity $v_z = 2.9 \text{ }\mu\text{m/s}$, therefore are mostly located in the lower part of the microchannel at the beginning of the experiment. As the ultrasound is switched on, some of the particles move to the pressure node, which in this configuration corresponds roughly to an horizontal plane located in the middle of the channel. In case of particles too close to the bottom wall, the radiation force is probably not strong enough to bring them up and they do not move. This behavior can clearly be observed in the lower plots of Fig. 2 showing the yz -position of the particles as a function of time. At the beginning of the experiment, the particles are uniformly distributed in the lower part of the channel, whereas at the end they are located either in the focal plane or at the bottom wall.

4. Discussion

The main aim of this experimental characterization was to estimate the acoustic energy density given at the different frequencies in the single-glass and double-glass zone. In order to have an acoustic trap, we need to achieve a difference in acoustic energy density between the double-glass and the single-glass zone. A first qualitative estimation of the acoustic energy density can be shown by plotting the z -position of the particle trajectories as a function of time for the different frequencies, as shown in Fig. 3. We consider now only particles with a depth position between -45 and 20 μm at $t = 0 \text{ s}$, highlighted in blue for the single-glass zone, and orange for the double-glass zone. It can be noticed that for $t < 0$ the particles are sinking with a constant velocity of approx 2.9 $\mu\text{m/s}$. As the ultrasound is switched on at $t = 0 \text{ s}$, the particles start to move toward the nodal plane, with a velocity proportional to the acoustic energy density. In general, the rising time of the particles in the single-glass region appears similar for all the frequencies, whereas in the double-glass region we observe that at $f = 3.356 \text{ MHz}$ the particles seem to have a much larger rising velocity, moving at the focal plane immediately after the ultrasound is turned on.

We then computed quantitatively the acoustic energy density E_{ac} by fitting the path $z(t)$ of each trajectory to the corresponding analytical expression (Bruus, 2012)

$$z(t) = \frac{1}{k} \arctan \left\{ \tan[kz(0)] \exp \left[\frac{4\Phi}{3} (ka)^2 \frac{E_{\text{ac}}}{\eta} t \right] \right\}, \quad (1)$$

with k the wave number, a the particle radius, Φ the acoustic contrast factor, η the dynamic viscosity of water. The results are presented in Fig. 4. It can be seen that there is a large variability of the measured E_{ac} , probably due to the fact that E_{ac} is not uniformly distributed across the channel. However, looking at the median values, the trend is very clear in the double-glass region, showing

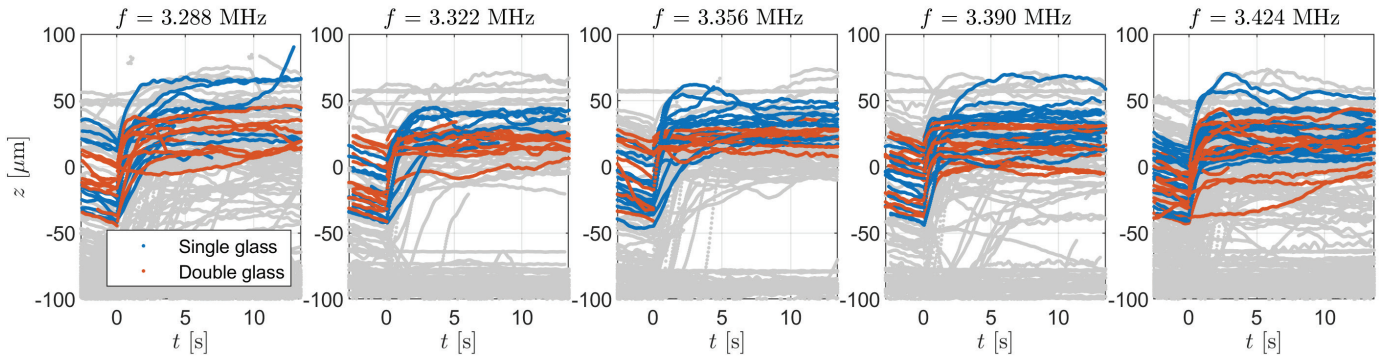


Figure 3. Focusing time for the different frequencies. The PZT transducer is switched on at $t = 0$. For $t < 0$, the polystyrene spheres sediment with a velocity of approximately $2.9 \mu\text{m/s}$. The acoustic energy density is calculated on trajectories with z -position at $t = 0$ between -45 and $20 \mu\text{m}$, highlighted in blue and orange for particles in the single-glass and double-glass zone, respectively.

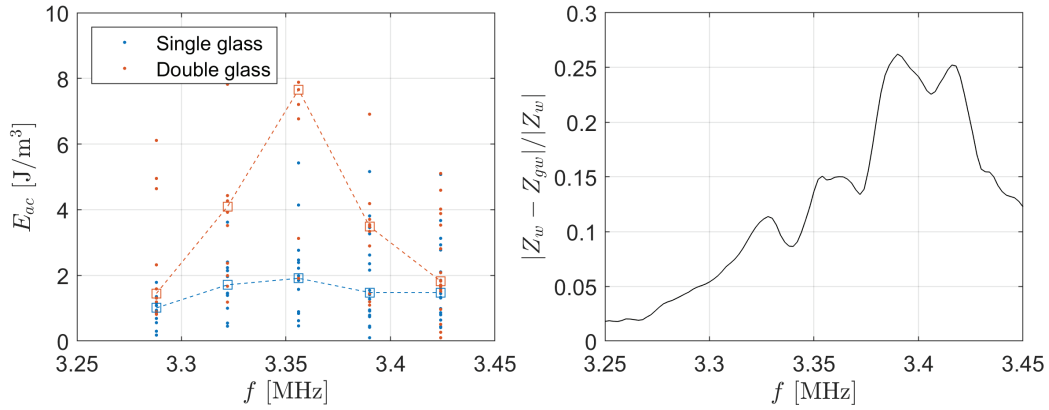


Figure 4. Left: acoustic energy density as a function of the actuation frequency for single-glass and double-glass region. Squared markers represent the median values. Right: Normalized differential impedance spectrum with the channel filled with water and a solution 10%-glycerol/water.

a maximum of $E_{ac} \approx 8 \text{ J/m}^3$ at $f = 3.356 \text{ MHz}$. Interestingly, that frequency is slightly lower than $f_{res} = 3.390 \text{ MHz}$, calculated using the differential impedance spectrum shown in the right plot of Fig. 4. On the other hand, the trend in the single-glass region is less clear, and the acoustic energy density is approximately the same for all frequencies around 2 J/m^3 . A possible explanation could be that the resonance frequency in this region is above the frequencies investigated.

5. Conclusions

We measured the 3D trajectories of $10\text{-}\mu\text{m}$ -diameter polystyrene beads inside a micro-acoustofluidic device using the General Defocusing Particle Tracking method. The thickness of the microchannel was locally modified by a double glass slide glued to the bottom wall, in order to induce a local change of the acoustic energy density in the device. We used the measured trajectories to estimate



the acoustic energy density in the single-glass and double-glass region. The results show a clear difference in the acoustic energy density of the two regions, suggesting that this approach could be used to realize acoustofluidic traps relying on geometrical modification of the channel.

Acknowledgements

MR acknowledges financial support by the Villum Foundation under the Grant No. 00036098. HB acknowledges financial support by the Villum Foundation under the Grant No. 00022951.

References

- Barnkob, R., Kähler, C. J., & Rossi, M. (2015). General defocusing particle tracking. *Lab on a Chip*, 15(17), 3556–3560.
- Barnkob, R., & Rossi, M. (2020). General defocusing particle tracking: fundamentals and uncertainty assessment. *Experiments in Fluids*, 61(4), 1–14.
- Barnkob, R., & Rossi, M. (2021). Defocustracker: A modular toolbox for defocusing-based, single-camera, 3d particle tracking. *Journal of Open Research Software*, 9(1), 22.
- Bruus, H. (2012). Acoustofluidics 7: The acoustic radiation force on small particles. *Lab on a Chip*, 12(6), 1014–1021.
- Cierpka, C., Rossi, M., Segura, R., & Kähler, C. (2011). On the calibration of astigmatism particle tracking velocimetry for microflows. *Measurement Science and Technology*, 22(1), 015401.
- Evander, M., Gidlöf, O., Olde, B., Erlinge, D., & Laurell, T. (2015). Non-contact acoustic capture of microparticles from small plasma volumes. *Lab on a Chip*, 15(12), 2588–2596.
- Karlsen, J. T., Qiu, W., Augustsson, P., & Bruus, H. (2018). Acoustic streaming and its suppression in inhomogeneous fluids. *Physical review letters*, 120(5), 054501.
- Lim, H. C., Soneji, S., Palmason, R., Lenhoff, S., Laurell, T., & Scheduling, S. (2021). Development of acoustically isolated extracellular plasma vesicles for biomarker discovery in allogeneic hematopoietic stem cell transplantation. *Biomarker research*, 9(1), 1–12.
- Muller, P. B., Rossi, M., Marin, A., Barnkob, R., Augustsson, P., Laurell, T., ... Bruus, H. (2013). Ultrasound-induced acoustophoretic motion of microparticles in three dimensions. *Physical Review E*, 88(2), 023006.
- Vitali, V., Core, G., Garofalo, F., Laurell, T., & Lenshof, A. (2019). Differential impedance spectra analysis reveals optimal actuation frequency in bulk mode acoustophoresis. *Scientific reports*, 9(1), 1–10.

